Mechanism of Carbon Dioxide-Catalyzed Oxidation of Tyrosine by Peroxynitrite[†]

Sergei V. Lymar, Qing Jiang, and James K. Hurst*

Department of Chemistry, Washington State University, Pullman, Washington 99163-4630

Received February 12, 1996; Revised Manuscript Received April 11, 1996[⊗]

ABSTRACT: Peroxynitrite ion (ONO_2^-) reacted rapidly with CO_2 to form a short-lived intermediate provisionally identified as the $ONO_2CO_2^-$ adduct. This adduct was more reactive in tyrosine oxidation than ONO_2^- itself and produced 3-nitrotyrosine and 3,3′-dityrosine as the major oxidation products. With tyrosine in excess, the rate of 3-nitrotyrosine formation was independent of the tyrosine concentration and was determined by the rate of formation of the $ONO_2CO_2^-$ adduct. The overall yield of oxidation products was also independent of the concentration of tyrosine and medium acidity; approximately 19% of the added ONO_2^- was converted to products under all reaction conditions. However, the 3-nitrotyrosine/3,3′-dityrosine product ratio depended upon the pH, tyrosine concentration, and absolute reaction rate. These data are in quantitative agreement with a reaction mechanism in which the one-electron oxidation of tyrosine by $ONO_2CO_2^-$ generates tyrosyl and NO_2 radicals as intermediary species, but are inconsistent with mechanisms that invoke direct electrophilic attack on the tyrosine aromatic ring by the adduct. Based upon its reactivity characteristics, $ONO_2CO_2^-$ has a lifetime shorter than 3 ms and a redox potential in excess of 1 V, and oxidizes tyrosine with a bimolecular rate constant greater than 2×10^5 M^{-1} s^{-1}. In comparison, in CO_2-free solutions, oxidation of tyrosine by peroxynitrite was much slower and gave significantly lower yields (∼8%) of the same products. When tyrosine was the limiting reactant, 3,5-dinitrotyrosine was found among the reaction products of the CO_2-catalyzed reaction, but this compound was not detected in the uncatalyzed reaction.

The peroxynitrite anion (ONO_2^-) and its conjugate peroxynitrous acid (ONO_2H) are powerful oxidants (Koppenol et al., 1992) that are under intensive scrutiny as possible pathogenic agents of human disease (Mulligan et al., 1991; Dawson et al., 1991; Moreno & Pryor, 1992; Beckman et al., 1993, 1994) and as deleterious oxidants associated with traumatic injury (Nowicki et al., 1991; Matheis et al., 1992; Szabo et al., 1995). Peroxynitrite is rapidly formed in aqueous solutions by addition of O_2^- and NO (Huie & Padmaja, 1993); consequently, biological tissues that simultaneously generate these species are putative sources of ONO_2^-. We have recently shown (Lymar & Hurst, 1995a) that ONO_2^- reacts rapidly with CO_2. Based upon the chemical nature of the reactants, the reaction is expected to produce an adduct, i.e.:

$$ONO_2^- + CO_2 \rightarrow ONO_2CO_2^- \qquad (1)$$

In the absence of other reactants, this adduct decomposes by hydrolysis to give bicarbonate (S. V. Lymar, unpublished observations) and nitrate ions (Uppu et al., 1996). Calculations based upon published rate data for reactions between peroxynitrite and various biological compounds indicate that reaction 1 will predominate in most biological fluids (Lymar & Hurst, 1996). Consequently, oxidative injury involving ONO_2^- is expected to occur primarily via the intermediacy of $ONO_2CO_2^-$. Thus, it is the chemical behavior of the adduct, rather than of ONO_2^- itself, that is most germane to the biomedical implications of *in vivo* formation of ONO_2^-.

Although ONO_2^- is highly toxic to *Escherichia coli* in CO_2-deficient *in vitro* bactericidal assays, addition of physiological levels of bicarbonate to the assay medium completely blocked killing under a wide range of conditions (Zhu et al., 1992; Lymar & Hurst, 1996). In contrast, ring nitration of aromatic compounds by peroxynitrite was catalyzed by CO_2 (Lymar & Hurst, 1995a; Uppu et al., 1996). Taken together, these results imply that $ONO_2CO_2^-$ is highly reactive, but also very short-lived, i.e., it decomposes before diffusing to cellular target sites (Wolcott et al., 1994; Lymar & Hurst, 1995b). To gain understanding of modulation of ONO_2^- reactivity by CO_2, we have undertaken a quantitative mechanistic study of CO_2-catalyzed oxidation of tyrosine. Our results, described herein, are in quantitative agreement with a mechanism in which the initial reaction step is one-electron oxidation of tyrosine producing tyrosyl and $^{\bullet}NO_2$ radicals, followed by reaction between these radicals, yielding 3-nitrotyrosine, and by tyrosine radical dimerization, forming 3,3′-dityrosine. The data are inconsistent with mechanisms involving direct nitration of the tyrosine aromatic ring by $ONO_2CO_2^-$ or isomeric secondary reactants derived from it (Uppu et al., 1996).

EXPERIMENTAL PROCEDURES

Reagents. L-Tyrosine, 3-nitrotyrosine, and all inorganic salts were the best-available grade from commercial suppliers and were used as received. Water was purified using a Milli-Q system. Stock peroxynitrite solutions were prepared from potassium nitrite and hydrogen peroxide (Keith & Powell, 1969). Residual H_2O_2 was decomposed by stirring the suspension for 10 min on ice with 1 mg/mL MnO_2 powder, and then centrifuging at 10000*g* and 0 °C for 15 min to remove MnO_2. Adventitious metal ions were removed by passing the solution through a 0.45 μm Bio-

[†] Financial support was provided by the National Institutes of Health under Grant AI-15834.

* To whom correspondence should be addressed.

[⊗] Abstract published in *Advance ACS Abstracts,* June 1, 1996.

S0006-2960(96)00331-5 CCC: $12.00

Rex 50W-X8 cation exchange membrane in Na^+ form. The ONO_2^- concentration was determined spectrophotometrically in alkaline solution using $\epsilon_{302} = 1.67 \times 10^3$ M^{-1} cm^{-1} (Hughes & Nicklin, 1968). Stock solutions were stored frozen at −80 °C for several months without noticeable decomposition. Standard 3,3′-dityrosine was prepared by horseradish peroxidase-catalyzed oxidation of tyrosine by H_2O_2 (Amado et al., 1984). The product gave a single spot ($R_f = 0.15$) on silica gel TLC in 4:1:1 butanol/acetic acid/H_2O. Buffers were prepared from sodium acetate or NaH_2PO_4; their pH values were adjusted with HCl. This procedure generated NaCl, but minimized contamination with carbonate, which is unavoidable if NaOH is used to adjust the buffers. When desired, buffers with pH below 7.5 were purged from carbonate by bubbling with argon for 30−40 min before using; carbonate absence was confirmed by measuring ONO_2^- lifetimes (Lymar & Hurst, 1995a).

Product Analyses. Reactions were initiated by flow-mixing equal volumes of solution using a manually driven two-syringe assembly connected to a 12-jet tangential mixer. One syringe contained tyrosine in either 0.3 M phosphate or 0.6 M acetate buffer and varying amounts of sodium bicarbonate; the pH was adjusted to give the desired final concentration of CO_2, assuming an equilibrium constant of 1.1×10^{-6} M for the reaction, $CO_2 + H_2O \rightleftharpoons H^+ + HCO_3^-$ (Harned & Bonner, 1945). The other syringe contained ONO_2^- in sodium hydroxide, the concentration of which (1−80 mM) was adjusted to give the desired pH in the mixed solutions. Under the experimental conditions, reaction 1 was much faster than CO_2 equilibration with HCO_3^-. Consequently, the CO_2 concentration during the reaction was fixed by the concentration in the reactant syringe, although the pH jumped to more alkaline values upon mixing. Flow-mixing was needed because reaction half-times were as short as 0.01 s. Peroxynitrite concentrations in syringe were measured within 10 s of mixing by transferring a portion to a cuvette and measuring the absorbance at 302 nm. Reactions were at ambient temperature (23 ± 1 °C). Products were analyzed by HPLC on a Gilson system with a 5 μm Spherisorb C-18 column and a UV/vis detector set at 276 nm. Three new peaks were detected and identified as 3-nitrotyrosine, 3,3′-dityrosine, and 3,5-dinitrotyrosine by absorption and fluorescence spectroscopy with HP 8452 diode array and PTI spectrophotometers and by NMR using a Bruker AMX-300 spectrometer. For the NMR measurements, HPLC peak fractions were collected, solvent was removed by rotovaporation, and the solid residues were dissolved in D_2O. ^1H NMR (300 MHz): for 3-nitrotyrosine, δ 2.98−3.14 (m, 2H), 3.82−3.86 (m, 1H), 7.04 (d, $J = 8.7$ Hz, 1H), 7.42 (dd, $J = 8.7$, 2.3 Hz, 1H), 7.90 (d, $J = 2.3$ Hz, 1H); for 3,5-dinitrotyrosine, δ 2.86−3.07 (m, 2H), 3.79−3.82 (m, 1H), 7.88 (s, 2H); for 3,3′-dityrosine, δ 2.96−3.09 (m, 5H), 3.80−3.84 (m, 2H), 6.86 (d, $J = 8.4$ Hz, 2H), 7.01 (d, $J = 2.25$ Hz, 2H), 7.08 (dd, $J = 8.4$, 2.25 Hz, 2H). Identities of 3-nitrotyrosine and 3,3′-dityrosine were confirmed by comparison of NMR spectra and by coelution with authentic samples. Yields of 3-nitrotyrosine were quantitated by comparison of HPLC peak areas with calibration curves constructed using known amounts of authentic samples. Yields of 3,3′-dityrosine were determined by collecting the eluted material, adjusting the pH of the fractions to 10.5, and comparing their fluorescence intensities at 410 nm (327 nm excitation) to the intensities of standard solutions of authentic material. Complete separation of 3,3′-dityrosine from tyrosine was not achieved. However, addition of excess tyrosine to the standard 3,3′-dityrosine solutions did not alter their fluorescence intensities, indicating that the presence of tyrosine did not affect the product yield measurements. Yields for each product are reported as the ratio of the product concentration to the concentration of added peroxynitrite.

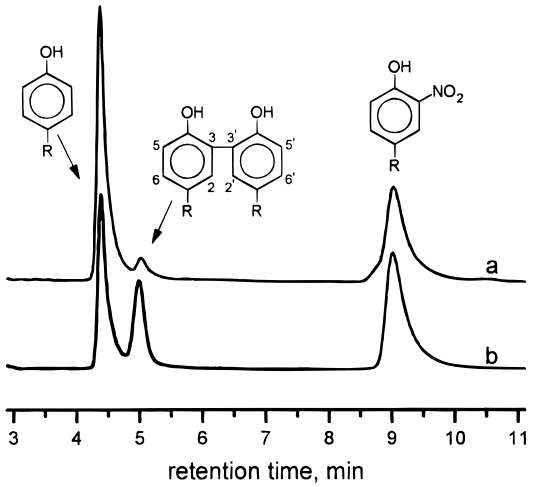

FIGURE 1: HPLC chromatogram of reaction products. Isocratic elution with 20 mM phosphate buffer, pH 3.0, plus 8% methanol. Trace a: product mixture from reaction between 200 μM ONO_2^- and 1 mM tyrosine in 0.15 M phosphate plus 25 mM carbonate, pH 7.5. Trace b: reference chromatogram containing 500 μM tyrosine (4.39 min), 67 μM 3,3′-dityrosine (5.00 min), and 33 μM 3-nitrotyrosine (9.03 min). Retention times are given in parentheses. The symbol R in the structures is $-CH_2CH(NH_3^+)CO_2^-$.

Kinetic Measurements. A thermostated Hi-Tech SF-40 stopped flow instrument was used for kinetic measurements. Peroxynitrite decay was monitored at 330 nm where interference from 3-nitrotyrosine is minimal; 3-nitrotyrosine formation was monitored at its spectral maximum of 422 nm. Kinetic calculations were performed as described in the text using Mathcad 4.0 software.

RESULTS

Identification of Reaction Products. When ONO_2^- was the limiting reagent, the same products were formed by reaction of ONO_2^- with tyrosine in CO_2-free and CO_2-containing media. A representative chromatogram is displayed in Figure 1. The two product peaks had the same retention times as 3,3′-dityrosine and 3-nitrotyrosine. The product with the retention time at ∼9 min exhibited absorption ($\lambda_{max} = 282$ and 422 nm (pH 11)) and ^1H NMR spectra that were identical to those of a 3-nitrotyrosine standard. The product with the retention time at ∼5 min exhibited absorption ($\lambda_{max} = 316$ nm (pH 11)), fluorescence ($\lambda_{ex} = 315$ nm, $\lambda_{em} = 410$ nm), and ^1H NMR spectra that were identical to those of a synthesized sample of 3,3′-dityrosine. When tyrosine was the limiting reagent (with ONO_2^- in 3−5-fold excess), 3,3′-dityrosine formation was not detected. Instead, in the presence of CO_2, an additional product was isolated by HPLC, which we tentatively assigned to 3,5-dinitrotyrosine on the basis of its ^1H NMR spectrum (Experimental Procedures). Specifically, a single peak was observed in the aromatic region of the spectrum whose chemical shift ($\delta = 7.88$) was very close to that for the proton adjacent to the NO_2 group in 3-nitrotyrosine. Both features are consistent

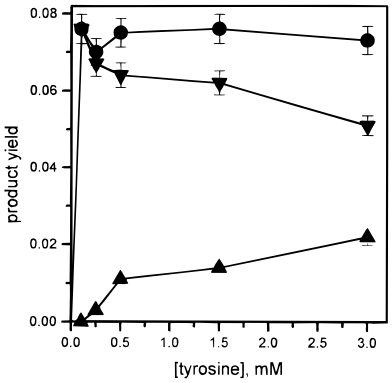

FIGURE 2: Dependence of yields of tyrosine oxidation products upon tyrosine concentration in CO_2-free solutions. Yields expressed as fractional conversion of ONO_2^- to products in 0.15 M phosphate, pH 7.5, where $[ONO_2^-] = 30-500\ \mu M$, subject to the condition that $[ONO_2^-] <$ [tyrosine]. Symbols: inverted triangles, 3-nitrotyrosine; triangles, 3,3′-dityrosine; circles, product sum. Estimated error limits based upon duplicate determinations are ±5% of the yield values.

with symmetric substitution in the 3- and 5-ring positions. Most of the mechanistic studies described below were performed using an excess of tyrosine over ONO_2^- to maintain nearly constant tyrosine concentrations over the reaction course. Under these conditions, 3,5-dinitrotyrosine was not formed. This product also did not form in CO_2-free solutions, even with ONO_2^- in severalfold excess.

Reaction in CO_2-Free Media. Formation of 3-nitrotyrosine and 3,3′-dityrosine in reaction of ONO_2^- with tyrosine has been previously reported (van der Vliet et al., 1994, 1995). Because it appears that no special precautions were taken in this work to avoid carbonate contamination of the reaction media, hence, catalysis by CO_2, we have reexamined aspects which are essential for direct comparison to the catalyzed reaction. The dependence of product yields upon tyrosine concentration in neutral solutions is illustrated in Figure 2. The total yield, expressed as fraction of ONO_2^- that forms products, was constant at ∼8% over the experimentally accessible tyrosine concentration range. However, the relative yield of 3-nitrotyrosine decreased with increasing tyrosine concentration, as previously noted (van der Vliet et al., 1995). Reaction half-times for ONO_2^- disappearance (Table 1, $t_{1/2}$ at 330 nm) and 3-nitrotyrosine formation (Table 1, $t_{1/2}$ at 422 nm) were nearly identical and independent of the tyrosine concentration. This indicates that product formation does not involve direct bimolecular reaction between ONO_2^- and tyrosine. No reaction was observed in alkaline solution (pH ≥11), implying that protonation of ONO_2^- is required for reactivity.

CO_2-Catalyzed Reactions. All experiments described in this section were performed with $[CO_2] \gg [ONO_2^-]$ in addition to [tyrosine] > $[ONO_2^-]$. Under these conditions, at least 95% of the added ONO_2^- disappeared via reaction 1 (Lymar & Hurst, 1995a). Phenomenologically, the major differences between the uncatalyzed and CO_2-catalyzed reactions were the much greater rates and product yields of tyrosine oxidation in the latter case. The total product yield first increased with increasing tyrosine concentrations, and then saturated at ∼19% (Figure 3). The plateau level attained was independent of medium acidity over the pH range 5−10 (Figure 4). In contrast, the yield of 3-nitrotyrosine relative to 3,3′-dityrosine (at a fixed tyrosine concentration) decreased

Table 1: Kinetic Data[a] for ONO_2^- Disappearance[b] and 3-Nitrotyrosine Formation[c]

[tyrosine] (mM)	$t_{1/2}$ (330 nm) (ms)	$t_{1/2}$ (422 nm) (ms)
Without Added Carbonate, pH 7.4		
0	4600	
0.1	4600	5000
2.0	4300	4300
With 20 mM Carbonate,[d] pH 7.4		
0	38	
0.1	38	41
2.0	35	36
With 25 mM Carbonate,[d] pH 9.7[e]		
0	15	
2.0	14	14
With 50 mM Carbonate,[d] pH 9.6[f]		
1.5	2.9	2.3

[a] In 0.15 M phosphate at 24 °C. [b] $t_{1/2}$ at 330 nm. [c] $t_{1/2}$ at 422 nm. [d] Analytical carbonate concentration, given as the sum $[CO_2] + [HCO_3^-] + [CO_3^{2-}]$. [e] pH-jump from pH 7.2. [f] pH-jump from pH 6.1.

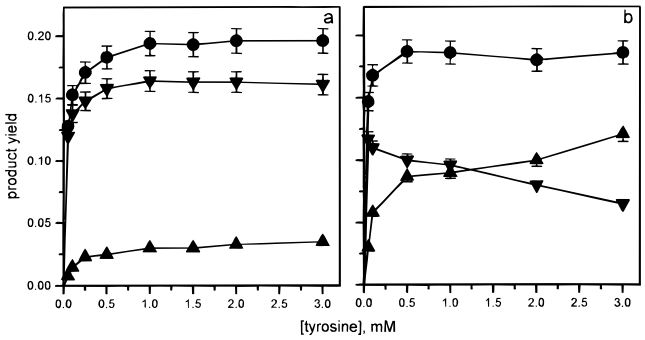

FIGURE 3: Dependence of yields of CO_2-catalyzed tyrosine oxidation products upon tyrosine concentration. Symbols and $[ONO_2^-]$ as in Figure 2; medium composition: 0.15 M phosphate plus 25 mM carbonate at pH 7.5 (panel a) or pH 8.7 (panel b). Data for panel b were obtained using pH-jump flow-mixing from pH 7.3 to satisfy the condition $[CO_2] \gg [ONO_2^-]$.

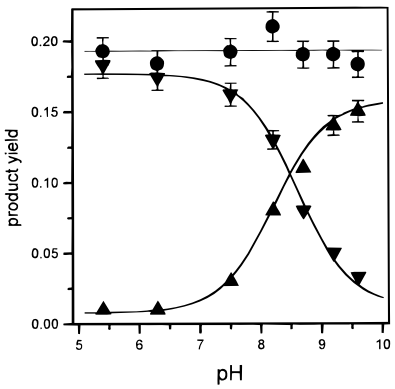

FIGURE 4: pH dependencies of the yields of CO_2-catalyzed tyrosine oxidation products. Symbols as in Figure 2. Reaction conditions: 2 mM tyrosine, 25 mM total carbonate, 0.5 mM ONO_2^- in 0.15 M phosphate; pH-jump flow-mixing from pH 7.3 was used for reactions at pH >7.6. As discussed in the text, the solid lines have no theoretical significance, but are presented only as visual aids.

with increasing solution alkalinity (Figures 3 and 4). To confirm that there were no other major products formed in this reaction, the decrease in tyrosine ($\Delta[\text{tyrosine}]_{exptl}$), measured directly from the tyrosine HPLC peak heights before and after reaction, was compared to the expected tyrosine consumption based upon experimentally determined product yields ($\Delta[\text{tyrosine}]_{calc}$), for which $\Delta[\text{tyrosine}]_{calc} =$ [3-nitrotyrosine] + 2[3,3′-dityrosine]. The comparison

showed that, under all conditions, greater than ~90% of the tyrosine that reacted formed these two products. For example, at pH 7.5, addition of 380 μM ONO_2^- to 1.1 mM tyrosine caused conversion of 95 μM tyrosine to 61 μM 3-nitrotyrosine and 11 μM 3,3′-dityrosine, yielding $\Delta[\text{tyrosine}]_{calc}/\Delta[\text{tyrosine}]_{exptl} = 0.87$, and addition of 600 μM ONO_2^- to 2.1 mM tyrosine caused conversion of 150 μM tyrosine to 96 μM 3-nitrotyrosine and 20 μM 3,3′-dityrosine, yielding $\Delta[\text{tyrosine}]_{calc}/\Delta[\text{tyrosine}]_{exptl} = 0.91$. At pH 9.3, addition of 480 μM ONO_2^- to 2.1 mM tyrosine caused conversion of 178 μM tyrosine to 26 μM 3-nitrotyrosine and 72 μM 3,3′-dityrosine, yielding $\Delta[\text{tyrosine}]_{calc}/\Delta[\text{tyrosine}]_{exptl} = 0.96$.

One potential complication is that the method used for preparing ONO_2^- yielded solutions that also contained nitrite ion, a known oxidant. Under the conditions employed, NO_2^- concentration levels as high as 0.5 mM could be attained in the final reaction medium. However, deliberate addition of up to 10 mM potassium nitrite to the reaction medium had no effect upon product yields or their distribution, indicating that NO_2^- was noninterfering.

Under most reaction conditions, the half-times for ONO_2^- disappearance and 3-nitrotyrosine formation were nearly identical. The rate of product formation was therefore determined by the rate of formation of $ONO_2CO_2^-$. Representative data, expressed as reaction half-times ($t_{1/2}$), are given in Table 1. At the fastest rates achievable (which are limited by the aqueous solubility of CO_2), the $t_{1/2}$ for 3-nitrotyrosine formation was consistently measured to be slightly smaller than the $t_{1/2}$ for ONO_2^- decay. This seemingly odd result is predicted by the mechanism proposed in the Discussion section. Although the total product yield did not change, the relative distribution between the two products depended also upon the absolute reaction rate. Specifically, increasing the rate by increasing the CO_2 concentration at constant ONO_2^- (Table 2, entries 1−5) or by increasing the ONO_2^- concentration at constant CO_2 (Table 2, entries 6−8) caused the relative amount of 3-nitrotyrosine formation to increase.

DISCUSSION

Redox Stoichiometry. The observations that the rates of reaction between ONO_2^- and tyrosine are independent of tyrosine concentration (Table 1) indicate that ONO_2^- itself is unreactive, but rather is a precursor to the actual reactant. Furthermore, since the maximal yields of products in the uncatalyzed and CO_2-catalyzed reactions are only 8% and 19%, respectively, of the added ONO_2^- (Figures 2−4), it is apparent that the reactive intermediates are formed only on the minor pathways of ONO_2^- decay. This conclusion is reached from the following arguments: Saturation of product yields at high tyrosine concentrations (Figures 2 and 3) implies complete capture of the reactive intermediate. Like any peroxide, ONO_2^- can be either a one-electron or two-electron oxidant. Both nitration and dimerization of tyrosine are two-electron oxidations. Thus, the reaction stoichiometry dictates that at most 16% and 38% of the added ONO_2^- is available for reaction with tyrosine in the uncatalyzed and catalyzed reactions, respectively. Reaction schemes accounting for this behavior require the presence of at least two intermediates, one reactive and the other unreactive toward tyrosine. As illustrated for the CO_2-catalyzed reaction, these intermediates can be formed either sequentially, as shown in Scheme 1, or concurrently, as shown in Scheme 2.

Scheme 1

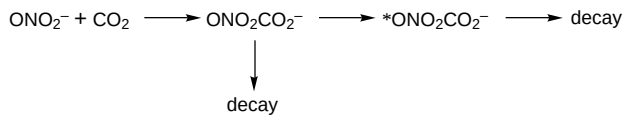

Scheme 2

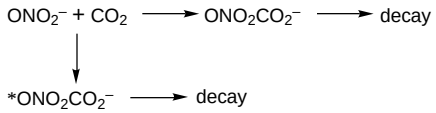

In Schemes 1 and 2, the reactive intermediate is indicated by the asterisk. Because the reaction half-time for 3-nitrotyrosine formation equals that for ONO_2^- decay, we conclude that the intermediates do not accumulate. Thus, for both schemes the rate-determining step is bimolecular reaction between ONO_2^- and CO_2. For the uncatalyzed reaction, similar schemes can be drawn with H^+ replacing CO_2 that involve partitioning between reactive and unreactive forms of ONO_2H. The ONO− group is more strongly electron withdrawing than the hydrogen atom (cf., ONO_2H ($pK_a = 6.6$) and HOH ($pK_a = 15.7$)). Consequently, ONO_2CO_2H is expected to be a stronger acid than carbonic acid ($HOCO_2H$, $pK_a \approx 3.6$), and the intermediate should be deprotonated under all conditions of this study.

Mechanism of CO_2-Catalyzed Tyrosine Oxidation. A mechanism that together with Scheme 1 or 2 accounts quantitatively for the data is given by the following reactions:

$$*ONO_2CO_2^- + \text{tyrosine} \rightarrow \text{tyr}^\bullet + {}^\bullet NO_2 + HCO_3^- \quad (2)$$

$$\text{tyr}^\bullet + \text{tyr}^\bullet \rightarrow \text{3,3′-dityrosine} \quad (3)$$

$$\text{tyr}^\bullet + {}^\bullet NO_2 \rightarrow \text{3-nitrotyrosine} \quad (4)$$

$${}^\bullet NO_2 + \text{tyrosine} \rightarrow NO_2^- + \text{tyr}^\bullet + H^+ \quad (5)$$

$${}^\bullet NO_2 + {}^\bullet NO_2 \xrightarrow{H_2O} NO_2^- + NO_3^- + 2H^+ \quad (6)$$

The symbol $\text{tyr}^\bullet$ indicates the tyrosyl radical, which is deprotonated above pH 0 (Dixon & Murphy, 1976). Step 2 constitutes one-electron oxidation of tyrosine to the radical by the reactive intermediate. Step 3 occurs during radiolysis of tyrosine (Hunter et al., 1989; Prutz et al., 1983), and steps 4 and 5 have been proposed as mechanistic steps in tyrosine nitration by $^\bullet NO_2$ (Prutz et al., 1985). Step 6 represents the well-described pathway for $^\bullet NO_2$ radical decay in aqueous solution (see, e.g., Huie, 1994) and is slow relative to reactions 3−5.

Qualitatively, our data can be understood in terms of the proposed mechanism as follows: First, the mechanism predicts that the total product yield depends only upon the amount of radicals formed in step 2. The experimental conditions were set to ensure that essentially all added ONO_2^- reacted with CO_2. Provided that the partitioning to $*ONO_2CO_2^-$ (see Schemes 1 and 2) is pH-independent and that sufficient tyrosine is present to capture all the $*ONO_2CO_2^-$ formed, the radical yield (and therefore the total product yield) will be invariant to reaction conditions. Second, the

Table 2: Dependence of [3-Nitrotyrosine]/[3,3′-Dityrosine] Ratios upon Reaction Conditions[a,b]

					product ratio[d]	
$[ONO_2^-]_0$ (μM)	[carbonate][c] (mM)	$t_{1/2}$ (330nm) (ms)	[3-nitrotyrosine] (μM)	[3,3′-dityrosine] (μM)	exptl	calcd
40	0.66	460	3.6	4.2	0.86	0.55
270	6.6	67	38	16	2.4	2.4
260	25	18	40	11	3.6	3.7
280	41	6.4	48	8.9	5.4	5.3
280	100	4.6	47	8.1	5.8	5.8
74	25	17	11	3.6	3.0	2.9
176	25	17	27	6.2	4.4	3.9
520	25	17	84	15	5.6	5.6

[a] In 0.15 M phosphate at 20 °C with [tyrosine] = 2.0 mM (entries 1−5) or at 23 °C with [tyrosine] = 1.5 mM (entries 6−8). [b] Reactions initiated with pH-jump from pH 7.0−7.2 to pH 7.5. [c] Analytical carbonate concentration, given as the sum $[CO_2] + [HCO_3^-] + [CO_3^{2-}]$. [d] Total product yield was 19−20% of added $[ONO_2^-]_0$.

yield of 3-nitrotyrosine relative to 3,3′-dityrosine depends upon the reaction conditions because these influence the relative contributions of steps 3−5 to the overall reaction. Specifically, the tyrosine phenolic group undergoes deprotonation in alkaline solution. Consequently, the rate constant for step 5 increases $\sim 10^2$-fold with increasing basicity over the range pH 7−11 (Prutz et al., 1985), whereas steps 3 and 4 are pH-independent. Step 5 is therefore a major sink for $^\bullet NO_2$ radicals under more alkaline conditions, leading to replacement of $^\bullet NO_2$ by tyr$^\bullet$, and thus increased formation of 3,3′-dityrosine at the expense of 3-nitrotyrosine. Since tyrosine is a reactant in step 5, increasing its concentration also favors replacement of $^\bullet NO_2$ by tyr$^\bullet$, accounting for the dependence of the product distribution upon tyrosine concentrations (Figure 3). The product ratio also depends upon the absolute reaction rate because this affects the partitioning of $^\bullet NO_2$ between steps 4 and 5. Specifically, increasing the reaction rate increases the transient concentration levels of the tyr$^\bullet$ and $^\bullet NO_2$ radicals. Because this also increases the [tyr$^\bullet$]/[tyrosine] ratio, a proportionately greater fraction of $^\bullet NO_2$ reacts via step 4, leading to an increased yield of 3-nitrotyrosine, as observed (Table 2). Finally, the smaller reaction half-time for 3-nitrotyrosine formation than for ONO_2^- disappearance that was measured for very rapid reactions (Table 1) has its origin in the decline in radical concentrations that occurs as the absolute reaction rate decreases over the reaction course. This leads to a shift away from 3-nitrotyrosine formation at the beginning of the reaction to increased 3,3′-dityrosine formation at the later stages. As the result, 3-nitrotyrosine formation decelerates more rapidly than ONO_2^- disappearance, which is reflected in the corresponding reaction half-times. This effect has been documented by the kinetic modeling described in the next paragraph. When the $t_{1/2}$ for ONO_2^- disappearance was 2.9 ms (Table 1, last entry), the calculated $t_{1/2}$ for 3-nitrotyrosine formation was 2.5 ms, as compared to a measured value of $t_{1/2} = 2.3$ ms. The proposed mechanism also explains why 3,3′-dityrosine formation is inefficient when $[ONO_2^-] \gg$ [tyrosine]. Under these conditions, tyrosine is rapidly consumed so that step 5 no longer contributes significantly to loss of $^\bullet NO_2$. Since the rate constant for step 4 is greater than the constant for step 3 (see below), the immediate reaction product is almost exclusively 3-nitrotyrosine; its subsequent nitration yields the observed 3,5-dinitrotyrosine.

The availability of rate constants for the individual reaction steps permitted quantitative evaluation of the proposed mechanism. The following equations were numerically integrated to give 3-nitrotyrosine/3,3′-dityrosine product ratios and $t_{1/2}$ values for 3-nitrotyrosine accumulation:

$$d[ONO_2^-]/dt = -k_1'[ONO_2^-]$$

$$d[tyr^\bullet]/dt = 0.19k_1'[ONO_2^-] - 2k_3[tyr^\bullet]^2 - k_4[tyr^\bullet][^\bullet NO_2] + k_5[^\bullet NO_2][\text{tyrosine}]_0$$

$$d[^\bullet NO_2]/dt = 0.19k_1'[ONO_2^-] - k_4[tyr^\bullet][^\bullet NO_2] - k_5[^\bullet NO_2][\text{tyrosine}]_0 - 2k_6[^\bullet NO_2]^2$$

$$d[\text{3-nitrotyrosine}]/dt = k_4[tyr^\bullet][^\bullet NO_2]$$

$$d[\text{3,3′-dityrosine}]/dt = k_3[tyr^\bullet]^2$$

Tyrosine and CO_2 were in sufficient excess over ONO_2^- for their concentrations to be treated as constant. Because sufficient tyrosine was present to trap all of the reactive intermediate ($^*ONO_2CO_2^-$) and because the rate-limiting step in the overall reaction was combination of ONO_2^- and CO_2, it follows that the rate of formation of tyrosyl and $^\bullet NO_2$ radicals in step 2 is independent of the tyrosine concentration and equal to the rate of disappearance of ONO_2^- multiplied by the fraction of ONO_2^- that forms $^*ONO_2CO_2^-$. Under all reaction conditions, this fraction was 0.19; the corresponding term for step 2 in the rate equations is therefore $0.19k_1'[ONO_2^-]$. The pseudo-first order rate constant for ONO_2^- decay (k_1') used in calculations was experimentally determined on the same solutions for which the product yields were measured. Values of the other rate constants were taken from the literature; these are as follows: $2k_3 = 4.2 \times 10^8$ M^{-1} s^{-1} (Prutz et al., 1983; Hunter et al., 1989), $k_4 = 3 \times 10^9$ M^{-1} s^{-1} (Prutz et al., 1985), and $2k_6 = 1.4 \times 10^8$ M^{-1} s^{-1} (Huie, 1994). The rate constant k_5 is pH-dependent; values of 3.2×10^5 M^{-1} s^{-1} at pH 7.5 and 7.5×10^6 M^{-1} s^{-1} at pH 9.6 were derived from published data (Prutz et al., 1985). Calculated [3-nitrotyrosine]/[3,3′-dityrosine] ratios accurately reproduced the measured ratios over a wide range of experimental conditions. Comparisons are given in Table 2 and Figure 5. The calculations also indicate that less than 5% of the $^\bullet NO_2$ disproportionate under the experimental conditions, confirming that step 6 contributed very little to the loss of oxidizing equivalents. Because independently determined rate constants for the individual reaction steps were utilized in the calculations, the close correspondence between predicted and observed product ratios provides strong support for the proposed mechanism.

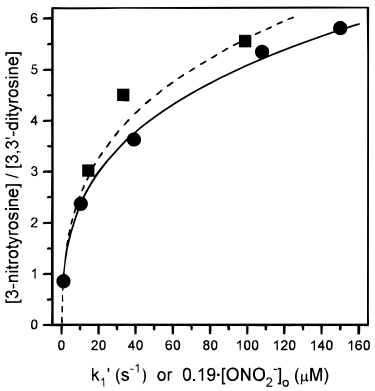

FIGURE 5: Comparison of predicted and experimentally determined product ratios upon reaction conditions. Circles: data from entries 1−5, Table 2; solid line: corresponding dependence upon k_1', calculated as described in the text from reaction steps 1−6, assuming an initial peroxynitrite concentration, $[ONO_2^-]_0 = 260$ μM. Squares: data from entries 6−8, Table 2; dashed line: corresponding calculated dependence upon $[ONO_2^-]_0$ for a fixed value of $k_1' = 40$ s^{-1}. Reaction conditions are given in Table 2.

Other researchers have suggested alternative mechanisms for aromatic nitration that do not involve radical intermediates. These mechanisms involve transfer of an activated NO_2 group from electrophilic intermediates (nitrocarboxylate, O_2NOCOR (Ischiropoulos et al., 1992), or nitrocarbonate, $O_2NOCO_2^-$ (Uppu et al., 1996)). As chemical analogs of acetyl nitrate (Schofield, 1980), these are plausible nitrating agents. However, these or any other mechanisms that invoke direct electrophilic attack of the aromatic ring by a nitrating agent cannot account for the dependence of the 3-nitrotyrosine/3,3′-dityrosine ratio upon the absolute reaction rate (Table 2 and Figure 5) and the more subtle effect that $t_{1/2}$ for 3-nitrotyrosine formation becomes smaller than $t_{1/2}$ for ONO_2^- decay at the highest reaction rates (Table 1). It was also suggested (Uppu et al., 1996) that, because the ortho/para (o/p) ratio of nitrophenols formed in the reaction of phenol with peroxynitrite did not change upon addition of CO_2, all nitration reactions involving ONO_2^- might be mediated by CO_2, even if present only as a contaminant. However, the radical mechanism described above predicts that reaction with ONO_2H and $*ONO_2CO_2^-$ will give the same o/p ratio because the isomeric product distribution is governed by radical coupling (e.g., step 4), which is independent of the identity of the radical-generating oxidant (e.g., step 2). Radical coupling following one-electron tyrosine oxidation by peroxynitrite has also been suggested for the uncatalyzed reaction (van der Vliet et al., 1995). These researchers also noted that the 3-nitrotyrosine/3,3′-dityrosine ratio declined if ONO_2^- was generated slowly by decomposition of 3-morpholinosydnonimine. This effect was attributed to reaction of tyrosyl radicals with O_2^-, an intermediary decomposition product. However, it is also consistent with our reaction mechanism because, as discussed above, slow formation of tyr$^\bullet$ will favor formation of 3,3′-dityrosine.

By analogy with the *in vitro* CO_2-catalyzed reaction, the extent of *in vivo* tyrosine nitration should depend upon both the total amount of $*ONO_2CO_2^-$ produced and its absolute rate of formation. When this rate is small, the efficiency of tyrosine nitration will be relatively low, and vice versa. The *in vivo* rate, in turn, will depend upon a variety of parameters, including the volume of the biological compartment where ONO_2^- is formed and the CO_2 concentration there; the latter is highly pH-dependent in the physiological range. Consequently, biological assays for nitrotyrosine might not serve as reliable indexes of the extent of peroxynitrite generation in tissues, particularly where comparisons are made between systems with differing reaction parameters (Lymar & Hurst, 1996). Caution should also be exercised in extrapolating *in vitro* results to reactions in biological environments, where conditions for tyrosine nitration are generally less favorable because the rate of generation is relatively small.

Nature of the Reactive Intermediate. Because tyrosine oxidation (step 2) occurs after the rate-determining step 1, little information on $*ONO_2CO_2^-$ can be obtained from kinetic studies. The $t_{1/2}$ for 3-nitrotyrosine formation was no larger than $t_{1/2}$ for ONO_2^- decay (Table 1), indicating that the intermediate did not accumulate. Consequently, the $*ONO_2CO_2^-$ lifetime must be significantly shorter than 3 ms, the smallest reaction half-time achieved in these studies (Table 1, last entry). Total yields of tyrosine oxidation saturated at less than 1 mM tyrosine under all reaction conditions (Figure 3), indicating that this concentration was sufficient to capture all of the $*ONO_2CO_2^-$ formed. Since these constraints require that $t_{1/2} \gg \ln 2/(k_2[\text{tyrosine}])$, the rate constant of step 2 must be $k_2 \gg 2 \times 10^5$ M^{-1} s^{-1}. The actual rate constant is probably pH-dependent because tyrosine is more easily oxidized when its phenolic group is deprotonated. Reported redox potentials are 1.2, 0.93, and 0.72 V at pH 2, 7, and 13, respectively (DeFelippis et al., 1991; Harriman, 1987). The fact that step 2 is rapid even at pH 5.5 suggests that the $*ONO_2CO_2^-$ redox potential exceeds 1 V.

In the absence of CO_2, the reactivity of peroxynitrite is thought to be dictated by partitioning between *cis* and *trans* rotameric states of ONO_2H, with the *trans* rotamer being more reactive (Koppenol et al., 1992; Tsai et al., 1994; Crow et al., 1994; Goldstein & Czapski, 1995; Pryor & Squadrito, 1995). It is possible that the reactive and unreactive forms of $ONO_2CO_2^-$ in Schemes 1 and 2 are analogous conformational states of the adduct, with CO_2 playing the same chemical role as the proton in activation of the oxidant. However, the species represented as $*ONO_2CO_2^-$ might equally well be secondary oxidants, for example, the $^\bullet NO_2$ and $^\bullet HCO_3$ radicals formed by cleavage of the peroxo O−O bond. Alternatively, the species represented as $ONO_2CO_2^-$ and $*ONO_2CO_2^-$ might be different structural isomers, e.g., $ONO_2CO_2^-$ and $O_2NOCO_2^-$. If only one of these isomers were capable of one-electron oxidation of tyrosine, it would constitute the reactive form of the adduct. At present, the available data are insufficient to permit definitive assignment of a structure to $*ONO_2CO_2^-$.

Although the pH dependencies for 3-nitrotyrosine and 3,3′-dityrosine formation (Figure 4) give the appearance of titration curves, these have nothing to do with protic equilibria involving the reaction intermediates. To the contrary, the overall yield of products was pH-independent, indicating that medium acidity did not affect the partitioning of the $ONO_2CO_2^-$ between reactive and unreactive forms (Schemes 1 and 2). The dependencies shown in Figure 4 reflect primarily an increase in the rate constant for step 5 accompanying deprotonation of the tyrosine phenolic group. However, other factors affecting the competition between steps 3−5 will also affect the product distribution. For example, the shapes of the curves on Figure 4 change

significantly if the product yields are determined at different concentrations of tyrosine or CO_2, or if different amounts of ONO_2^- are used. This behavior clearly illustrates the pitfalls associated with assigning pK_a values to proposed intermediates from product yield data where reaction mechanisms have not been established, and may be important to current discussions of intermediates formed from ONO_2^- based upon pH dependencies of product yields (Crow et al., 1994; Pryor & Squadrito, 1995).

ACKNOWLEDGMENT

The authors are grateful to Scot Wherland for providing access to his stopped flow instrument, to John W. Coddington for a gift of active MnO_2, and to James D. Satterlee and Steven F. Sukits for assistance in acquiring the NMR data.

REFERENCES

Amado, R., Aeschbach, R., & Neukom, H. (1984) *Methods Enzymol. 107*, 377−388.
Beckman, J. S., Carson, M., Smith, C. D., & Koppenol, W. H. (1993) *Nature 346*, 584.
Beckman, J. S., Ye, Y. Z., Anderson, P. G., Chen, J., Accavitti, M. A., Tarpey, M. M., & White, C. R. (1994) *Biol. Chem. Hoppe-Seyler 375*, 81−88.
Crow, J. P., Spruell, C., Chen, J., Gunn, C., Ischiropoulos, H., Tsai, M., Smith, C. D., Radi, R., Koppenol, W. H., & Beckman, J. S. (1994) *Free Radical Biol. Med. 16*, 331−338.
Dawson, V. L., Dawson, T. M., London, E. D., Bredt, D. S., & Snyder, S. H. (1991) *Proc. Natl. Acad. Sci. U.S.A. 88*, 6368−6371.
DeFelippis, M. R., Murthy, C. P., Broitman, F., Weinraub, D., Faraggi, M., & Klapper, M. H. (1991) *J. Phys. Chem. 95*, 3416−3419.
Dixon, W. T., & Murphy, D. (1976) *J. Chem. Soc., Faraday Trans. 2 72*, 1221−1230.
Goldstein, S., & Czapski, G. (1995) *Inorg. Chem. 34*, 4041−4048.
Harned, H. C., & Bonner, F. C. (1945) *J. Am. Chem. Soc. 67*, 1026−1031.
Harriman, A. (1987) *J. Phys. Chem. 91*, 6102−6104.
Hughes, M. N., & Nicklin, H. G. (1968) *J. Chem. Soc. (A) 1968*, 450−452.
Huie, R. E. (1994) *Toxicology 89*, 193−216.
Huie, R. E., & Padmaja, S. (1993) *Free Radical Res. Commun. 18*, 195−199.
Hunter, E. P. L., Desrosiers, M. F., & Simic, M. G. (1989) *Free Radical Biol. Med. 6*, 581−585.
Ischiropoulos, H., Zhu, L., Chen, J., Tsai, M., Martin, J. C., Smith, C. D., & Beckman, J. S. (1992) *Arch. Biochem. Biophys. 298*, 431−437.
Keith, W. G., & Powell, R. E. (1969) *J. Chem. Soc. (A) 1969*, 90.
Koppenol, W. H., Moreno, J. J., Pryor, W. A., Ischiropoulos, H., & Beckman, J. S. (1992) *Chem. Res. Toxicol. 5*, 834−842.
Lymar, S. V., & Hurst, J. K. (1995a) *J. Am. Chem. Soc. 117*, 8867−8868.
Lymar, S. V., & Hurst, J. K. (1995b) *Chem. Res. Toxicol. 8*, 833−840.
Lymar, S. V., & Hurst, J. K. (1996) *Chem. Res. Toxicol.*, in press.
Matheis, G., Sherman, M. P., Buckberg, G. D., Haybron, D. E., Young, H. H., & Ignarro, L. J. (1992) *Am. J. Physiol. 262*, H616−H620.
Moreno, J. J., & Pryor, W. A. (1992) *Chem. Res. Toxicol. 5*, 425−431.
Mulligan, M. S., Hevel, J. M., Marletta, M. A., & Ward, P. A. (1991) *Proc. Natl. Acad. Sci. U.S.A. 88*, 6338−6342.
Nowicki, J. P., Duval, D., Poignet, H., & Scratton, B. (1991) *Eur. J. Pharmacol. 204*, 339−340.
Prutz, W. A., Butler, J., & Land, E. J. (1983) *Int. J. Radiat. Biol. 4*, 183−196.
Prutz, W. A., Monig, H., Butler, J., & Land, E. J. (1985) *Arch. Biochem. Biophys. 243*, 125−134.
Pryor, W. A., & Squadrito, G. L. (1995) *Am. J. Physiol. 268*, L699−L722.
Schofield, K. (1980) *Aromatic Nitration*, Cambridge University Press, Cambridge, England.
Szabo, C., Salzman, A. L., & Ischiropoulos, H. (1995) *FEBS Lett. 372*, 229−232.
Tsai, J.-H., M., Harrison, J. G., Martin, J. C., Hamilton, T. P., van der Woerd, M., Jablonsky, M. J., & Beckman, J. S. (1994) *J. Am. Chem. Soc. 116*, 4115−4116.
Uppu, R. M., Squadrito, G. L., & Pryor, W. A. (1996) *Arch. Biochem. Biophys. 327*, 335−343.
van der Vliet, A., O'Neill, C. A., Halliwell, B., Cross, C. E., & Kaur, H. (1994) *FEBS Lett. 339*, 89−92.
van der Vliet, A., Eiserich, J. P., O'Neill, C. A., Halliwell, B., & Cross, C. E. (1995) *Arch. Biochem. Biophys. 319*, 341−349.
Wolcott, R. G., Franks, B. S., Hannum, D. M., & Hurst, J. K. (1994) *J. Biol. Chem. 269*, 9721−9728.
Zhu, L., Gunn, C., & Beckman, J. S. (1992) *Arch. Biochem. Biophys. 298*, 452−457.

BI960331H